

CONTROL VOLUME APPROXIMATION OF DEGENERATE
TWO-PHASE POROUS FLOWS*

THOMAS J. MURPHY† AND NOEL J. WALKINGTON‡

Abstract. Implicit Euler approximations of the equations governing the porous flow of two immiscible incompressible fluids are shown to be the Euler–Lagrange equations of a convex function. Tools from convex analysis are then used to develop robust fully discrete algorithms for their numerical approximation. Existence and uniqueness of solutions to control volume approximations are established.

Key words. degenerate, two-phase flow, convexity

AMS subject classifications. 65N12, 76S05

DOI. 10.1137/17M1160744

1. Introduction. Numerical approximation of the equations modeling the flow of two incompressible immiscible fluids in a porous medium $\Omega \subset \mathbb{R}^d$ with $d = 2$ or 3 is considered. These equations take the form of conservation laws for the balance of mass of each fluid; let ρ_π , $\pi = 1, 2$, denote the mass of each fluid per unit volume¹ of Ω ,

$$\frac{\partial \rho_\pi}{\partial t} + \operatorname{div}(\rho_\pi \mathbf{v}_\pi) = q_\pi \quad \text{in } (0, T) \times \Omega.$$

The velocities are determined from Darcy laws $\mathbf{v}_\pi = K_\pi(\mathbf{b}_\pi - \nabla p_\pi)$ with body (gravity) forces \mathbf{b}_π , and the phase pressures p_π are determined from the incompressibility condition and a capillary pressure relation for the difference $p_1 - p_2$. Since the fluids are incompressible it is traditional to write $\rho_\pi = \tilde{\rho}_\pi s_\pi$, where $\tilde{\rho}_\pi$ is constant (the mass density of fluid π) and s_π is the saturation (volume of fluid π per unit volume of Ω).

These equations exhibit significant degeneracy in the spatial terms when one fluid is not present or displaces another ($\rho_\pi = 0$), or becomes immobile below a certain saturation ($\mathbf{v}_\pi = 0$). The incompressibility constraint gives rise to an additional degeneracy in the temporal term since the densities (ρ_1, ρ_2) are not a bijective function of the pressures (p_1, p_2) . In addition, if the porosity of the medium vanishes (or is small) in a portion of the domain Ω , the densities ρ_π vanish.

Below it is shown that implicit Euler approximations of these equations can be cast as convex minimization problems. Implicit Euler approximations of the pair of equations (the simultaneous solution method [11]) were considered by Douglas, Peaceman, and Rachford [16] in 1959; however, to date the convex structure has not been exploited in a numerical context. The following statement from the survey article [30] by Rockafellar well illustrates the need to rectify this omission.

*Received by the editors December 11, 2017; accepted for publication (in revised form) January 11, 2019; published electronically March 14, 2019.

<http://www.siam.org/journals/sinum/57-2/M116074.html>

Funding: The work of the second author was supported in part by National Science Foundation grants DMS-1418991 and DREF-1729478 as well as the NSF through the Center for Nonlinear Analysis.

[†]Department of Mathematical Sciences, Carnegie Mellon University, Pittsburgh, PA 15213 (exp90@mail.com, noelw@cmu.edu).

¹Frequently the density is defined to be mass per unit pore volume of Ω . This is poorly defined in regions where the pore volume vanishes (or is small).

In fact the great watershed in optimization isn't between linearity and nonlinearity, but convexity and nonconvexity. Even for problems that aren't themselves of convex type, convexity may enter, for instance, in setting up subproblems as part of an iterative numerical scheme.

Below tools from convex analysis are utilized to address the following fundamental issues:

- Existence and stability is established for a broad class of fully discrete schemes for the two-phase problem.
- A detailed analysis of the control volume scheme is presented for which the degeneracies can be completely characterized.
- Schemes for the minimization of degenerate convex problems are considered, and a numerical example presented.

1.1. Background. Porous flow of two immiscible incompressible fluids models the most easily implemented enhanced oil recovery process. For this reason these equations and their numerical simulation have been intensely studied in both the engineering and mathematical communities over the past half century, giving rise to a vast body of literature on the topic. In this section we limit the scope of the discussion to the mathematical structure of these equations and the structural properties of numerical schemes associated with the degenerate nature of these problems. The text by Rivière [29] contains a concise synopsis of the two-phase problem, and the monographs [8, 11] provide a comprehensive introduction to both the physical models and the numerical schemes for this problem.

Existence of solutions to the degenerate two-phase problem was established by Kroener and Luckhaus [21] and Alt and DiBenedetto [1]. Essentially all existence results for this problem are established under the assumption that the permeability matrix K_π of a phase only vanishes when the saturation of the phase vanishes (the partially degenerate case below). This precludes the situation where one phase can completely displace the other [29]. A common approach for establishing existence of solutions is to observe that upon adding the equations for each phase the sum of the temporal derivatives vanishes since the fluids are incompressible. This gives an equation of the form

$$\operatorname{div}(s_1 \mathbf{v}_1 + s_2 \mathbf{v}_2) = q_1 + q_2.$$

It is frequently possible to introduce an enigmatic change of variables [1, 2, 9] to get $s_1 \mathbf{v}_1 + s_2 \mathbf{v}_2 = \lambda \nabla p$, which results in an elliptic equation for (the “total pressure”) p . The two-phase problem can then be cast as an elliptic equation coupled to a parabolic problem. In general, numerical schemes for the two-phase problem pose the problem as either two conservation laws (the simultaneous solution method) [16, 32] or a single conservation law coupled to an elliptic equation for the total pressure [3, 7, 10, 12, 18, 26, 28, 36]. More recently alternative formulations of the two-phase problem [6] have been proposed which extend the ideas developed for the one-phase problem in [20, 25].

In order to circumvent degeneracies in the temporal term due to the incompressibility constraint, it is frequently assumed that the fluids are slightly compressible for both the one- and two-phase problems, in the mathematical and numerical works, e.g., [17, 19]. Posing the problem with saturations (densities) defined to be the volume (mass) of a phase per unit volume of Ω eliminates many of the difficulties associated with incompressibility. In this context the incompressibility constraint becomes $s_1 + s_2 = 1 - s_0$, where $s_0 : \Omega \rightarrow [0, 1]$ is the saturation of the medium [1, 33]. At points where $s_0(x) = 1$ it is immediate that $s_1 = s_2 = 0$ and the saturations are deter-

mined by the constraint. Numerical approximation of nonnegative variables subject to linear constraints is a classical topic and easily accommodated in this context.

2. Two-phase problem. In this section the equations modeling the porous flow of two immiscible incompressible fluids are presented and their convexity properties developed. Degeneracy can preclude rigorous derivations, so the presentation in this section is formal. In the next section finite dimensionality allows a rigorous treatment of the control volume scheme.

2.1. Classical formulation. When the fluids are incompressible, the mass per unit volume of the medium takes the form $\rho_\pi = \tilde{\rho}_\pi s_\pi$, where $\tilde{\rho}_\pi > 0$ is constant and $s_\pi = s_\pi(t, x)$ is the saturation, i.e., volume of fluid π per unit volume of Ω . The classical statement of the equations for the balance of mass for each phase then takes the form

$$(2.1) \quad \frac{\partial s_\pi}{\partial t} - \operatorname{div}(K_\pi(\mathbf{s})(\nabla p_\pi - \mathbf{b}_\pi)) = 0, \quad \pi = 1, 2,$$

where the following hold:

- $K_\pi(\mathbf{s}) = s_\pi k_\pi(\mathbf{s}) K_0 / \mu_\pi$, where $K_0 : \Omega \rightarrow \mathbb{R}^{d \times d}$ is the symmetric positive definite permeability matrix of the medium, $\mu_\pi \in (0, \infty)$ is the viscosity, and $k_\pi(\mathbf{s}) = k_\pi(x, \mathbf{s}) \geq 0$ is the relative permeability of phase π . The latter characterizes the flow properties of the fluid when other fluids are present; Figure 2.1 illustrates prototypical curves for these coefficients. Note that $K_\pi = 0$ when $s_\pi = 0$, so degeneracy of the equations is unavoidable.
- \mathbf{b}_π are the external body forces (force per unit volume). Typically $\mathbf{b}_\pi = \rho_\pi \mathbf{g}$, where \mathbf{g} is the gravitational force per unit mass; however, they may depend explicitly upon (t, x) and (s_1, s_2) or the pressures.
- The incompressibility constraint then becomes $s_0 + s_1 + s_2 = 1$, where $s_0 : \Omega \rightarrow [0, 1]$ is the saturation (volume ratio) of the medium so that $1 - s_0$ is the porosity. Also, implicit in this formulation are the constraints that the saturations must be nonnegative.
- The phase pressures take the form $p_1 = p + p_c$ and $p_2 = p - p_c$ where p is the Lagrange multiplier dual to the incompressibility constraint, and $p_c = p_c(x, \mathbf{s})$ is the capillary pressure which characterizes the surface tension and wetting properties of the fluid.
- Equation (2.1) does not include terms modeling mass sources and sinks. Naive inclusion of a nonhomogeneous term on the right-hand side is not meaningful in the current setting since the left-hand side vanishes in degenerate regions.

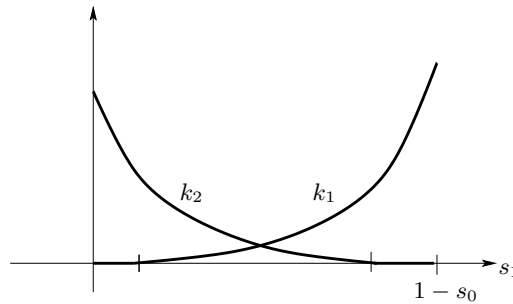


FIG. 2.1. *Prototypical relative saturation curves.*

Clearly solutions will not exist if, for example, a source term is introduced which extracts fluid from a region where none is present or injects fluid into a saturated impervious region.

In section 4 we discuss the additional terms typically included in the mass balances (2.1) to model wells where fluids are injected and/or extracted and how their presence impacts the existence and uniqueness properties of the solutions.

Equations (2.1) and the two constraints $s_0 + s_1 + s_2 = 1$ and $p_1 - p_2 = 2p_c$ give four equations for the four variables (s_1, s_2, p_1, p_2) .

NOTATION 2.1. Below $\mathbf{p} = (p_1, p_2)$ will denote the pair of pressures and $\mathbf{s} = (s_1, s_2)$ the pair of saturations.

2.2. Convex structure. The capillary pressure is a monotone increasing function of the difference $s_1 - s_2$, so can be realized as the derivative of a convex² function $\tilde{\gamma} : [-1 + s_0, 1 - s_0] \rightarrow \mathbb{R}$ of the difference, $p_c(\mathbf{s}) = \tilde{\gamma}'(s_1 - s_2)$. More generally, $p_\pi = p + \partial e_I / \partial s_\pi$ where $e_I = e_I(\mathbf{s})$ is a convex function modeling the energy (per unit volume of Ω) of the interfaces between the fluids (surface tension) and of the interfaces between the fluids and medium (wetting).

The pressure–saturation relation at each point $x \in \Omega$ can be written as $\mathbf{p} = \partial(I_L + \Gamma)(\mathbf{s})$, where $I_L, \Gamma : \mathbb{R}^2 \rightarrow \mathbb{R} \cup \{\infty\}$ are the convex functions $\Gamma(\mathbf{s}) = \gamma(s_1 - s_2)$ and

$$I_L(\mathbf{s}) = \begin{cases} 0, & s_1 + s_2 = 1 - s_0(x), \\ \infty & \text{otherwise} \end{cases} \quad \text{with } \gamma(s_1 - s_2) \equiv \begin{cases} \tilde{\gamma}(s_1 - s_2), & |s_1 - s_2| \leq 1 - s_0(x), \\ \infty & \text{otherwise}, \end{cases}$$

and $\partial(I_L + \Gamma)$ denotes the subgradient (at each point $x \in \Omega$). Here I_L is the indicator function of the set $L = \{\mathbf{s} \in \mathbb{R}^2 \mid s_1 + s_2 = 1 - s_0\}$ which enforces the equality constraint, and Γ is the sum of the surface tension function and the indicator of the set $\{\mathbf{s} \in \mathbb{R}^2 \mid |s_1 - s_2| \leq 1 - s_0\}$ which guarantees nonnegativity of saturations on the set L .

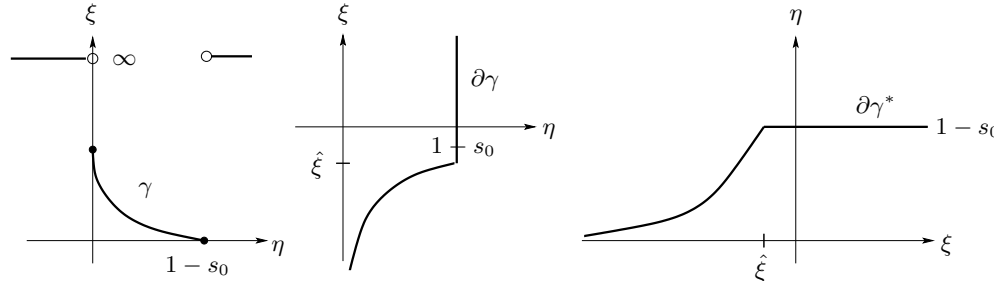


FIG. 2.2. Prototypical interfacial energy; $\eta \equiv (1 - s_0 + s_1 - s_2)/2 \in [0, 1 - s_0]$.

Expanding the definition of the subgradient shows that (see Figure 2.2)

$$\begin{pmatrix} p_1 \\ p_2 \end{pmatrix} \in p \begin{pmatrix} 1 \\ 1 \end{pmatrix} + (1/2)\partial\gamma(s_1 - s_2) \begin{pmatrix} 1 \\ -1 \end{pmatrix}.$$

The inverse saturation–pressure relation is realized as $\mathbf{s} \in \partial(I_L + \Gamma)^*(\mathbf{p})$, where

$$(I_L + \Gamma)^*(\mathbf{p}) = \sup_{\mathbf{s} \in \mathbb{R}^2} (\mathbf{p} \cdot \mathbf{s} - (I_L + \Gamma)(\mathbf{s}))$$

²In the engineering literature the capillary pressure takes the opposite sign. With the choice of sign utilized here, p_c can be realized as the derivative of a convex rather than a concave function.

is the convex conjugate of $I_L + \Gamma$. A calculation shows that

$$(2.2) \quad \begin{pmatrix} s_1 \\ s_2 \end{pmatrix} = \begin{pmatrix} 0 \\ 1 - s_0 \end{pmatrix} + (\gamma^*)'(p_1 - p_2) \begin{pmatrix} 1 \\ -1 \end{pmatrix}.$$

For the porous flow problem γ is smooth on its domain, which is bounded, so γ^* is finite on all of the real line and is differentiable, $\partial\gamma^* = (\gamma^*)'$.

Example. A prototypical Brooks–Corey capillary pressure [4, 29] takes the form $p_c(\mathbf{s}) = -1/(2\sqrt{s_1})$. Note that $s_1 = (1 - s_0 + s_1 - s_2)/2 \equiv \eta$ when $s_0 + s_1 + s_2 = 1$. Then with $\hat{\xi} \equiv -1/(2\sqrt{1 - s_0})$,

$$\gamma(\eta) = \sqrt{1 - s_0} - \sqrt{\eta} + I_{[0,1-s_0]}(\eta), \quad \partial\gamma(\eta) = \begin{cases} -1/(2\sqrt{\eta}), & \eta \in (0, 1 - s_0), \\ [\hat{\xi}, \infty), & \eta = 1 - s_0, \end{cases}$$

where $I_{[0,1-s_0]}$ is the indicator function of the interval $[0, 1 - s_0]$. The conjugate function and its derivative are

$$\gamma^*(\xi) = \begin{cases} -\sqrt{1 - s_0} - 1/(4\xi), & \xi \in (-\infty, \hat{\xi}], \\ (1 - s_0)\xi, & \xi \in [\hat{\xi}, \infty), \end{cases} \quad \partial\gamma^*(\xi) = \begin{cases} \frac{1}{4\xi^2}, & \xi \in (-\infty, \hat{\xi}], \\ 1 - s_0, & \xi \in [\hat{\xi}, \infty). \end{cases}$$

These functions take the form shown in Figure 2.2. In general $s_0 = s_0(x)$, so γ may depend explicitly upon $x \in \Omega$. Since this does not influence the analysis below, the dependence upon x will not be exhibited in the notation. ■

Using equations (2.2), eliminating the saturations from equations (2.1) gives a coupled pair of degenerate diffusion equations for the pressures. Initial data for these equations would be the saturations at time $t = 0$, and the natural no-flux boundary conditions take the form $K_\pi \nabla p_\pi = K_\pi \mathbf{b}_\pi$. Under mild regularity assumptions, the chain rule for subgradients [35] states that

$$\mathbf{p} \in \partial(I_L + \Gamma)(\mathbf{s}) \quad \Rightarrow \quad (\mathbf{s}_t, \mathbf{p}) = \frac{d}{dt}(I_L + \Gamma)^*(\mathbf{p}),$$

so the natural a priori estimate for (2.1)–(2.2) with no-flux boundary data is

$$(2.3) \quad \int_{\Omega} \gamma^*(\mathbf{p}(t)) + \int_0^t \int_{\Omega} \sum_{\pi=1}^2 |\nabla p_\pi|_{K_\pi}^2 = \int_{\Omega} \gamma^*(\mathbf{p}(0)) + \int_0^t \int_{\Omega} \sum_{\pi=1}^2 (\mathbf{b}_\pi, \nabla p_\pi)_{K_\pi}.$$

Here $(\mathbf{p}, \mathbf{q})_{K_\pi} = K_\pi \mathbf{p} \cdot \mathbf{q}$ is the inner product on pairs induced by K_π , and we write $\gamma^*(\mathbf{p}) \equiv \gamma^*(p_1 - p_2)$.

2.3. Implicit Euler approximation. Letting $\tau > 0$ denote a time step, the implicit Euler approximation of (2.1) and (2.2) becomes

$$(2.4) \quad s_\pi^n - s_\pi^{n-1} - \tau \operatorname{div}(K_\pi^{n-1}(\nabla p_\pi^n - \mathbf{b}_\pi^{n-1})) = 0, \quad \mathbf{s}^n \in \partial(I_L + \Gamma)^*(\mathbf{p}^n).$$

In these expressions the superscript indicates the temporal index, $s_\pi^n \simeq s_\pi(n\tau)$ and $K_\pi^{n-1} = K_\pi(\mathbf{s}^{n-1})$, $\mathbf{b}_\pi^{n-1} = \mathbf{b}_\pi(\mathbf{s}^{n-1})$, etc. Solutions of this scheme with no-flux boundary conditions are minimizers of

$$(2.5) \quad \Psi(\mathbf{p}) = \int_{\Omega} \left\{ \gamma^*(p_1 - p_2) - s_1^{n-1}(p_1 - p_2) + \frac{\tau}{2} \sum_{\pi=1}^2 |\nabla p_\pi - \mathbf{b}_\pi^{n-1}|_{K_\pi^{n-1}}^2 \right\}.$$

Convexity of γ^* guarantees

$$(\gamma^*)'(p_1^n - p_2^n) ((p_1^n - p_2^n) - (p_1^{n-1} - p_2^{n-1})) \geq \gamma^*(p_1^n - p_2^n) - \gamma^*(p_1^{n-1} - p_2^{n-1}),$$

from which the discrete analogue of (2.3) for solutions of the implicit Euler scheme (2.4) follows:

$$\int_{\Omega} \gamma^*(\mathbf{p}^n) + \tau \sum_{m=1}^n \int_{\Omega} \sum_{\pi=1}^2 |\nabla p_{\pi}^m|_{K_{\pi}^{m-1}}^2 \leq \int_{\Omega} \gamma^*(\mathbf{p}^0) + \tau \sum_{m=1}^n \int_{\Omega} \sum_{\pi=1}^2 (\nabla p_{\pi}^m, \mathbf{b}_{\pi}^{m-1})_{K_{\pi}^{m-1}}.$$

2.4. Degeneracy. The natural space of functions for which $\Psi(\mathbf{p})$ is finite is

$$U^{n-1} = \left\{ \mathbf{p} \in L^1(\Omega)^2 \mid \int_{\Omega} \sum_{\pi=1}^2 |\nabla p_{\pi}|_{K_{\pi}^{n-1}}^2 < \infty \right\};$$

however, while the permeabilities K_{π}^{n-1} are typically bounded, they may vanish on large subsets of Ω . In particular, the spatial term in Ψ is not strictly convex so minimizers are not unique; for example, p_{π} is undefined when a phase vanishes. In addition, properties typically available for Sobolev functions, such as trace theorems, are not available. Nonuniqueness also arises due to the no-flux boundary condition and saturation of the pores by one fluid; specifically, we have the following:

1. $\Psi(\mathbf{p})$ is unchanged upon shifting both pressures by the same constant, $(p_1, p_2) \mapsto (p_1 + c, p_2 + c)$. As for the classical Neumann problem, this degeneracy may be eliminated by working on the subspace of functions for which the average of $p_1 + p_2$ vanishes.
2. If $\hat{\xi} = \hat{\xi}(x) \in \mathbb{R}$ is the first point where $(\gamma^*)'(\xi)$ attains its maximal value of $1 - s_0$, the pressure difference $p_1 - p_2$ is not determined by the surface tension when $p_1 - p_2 - \hat{\xi} \geq 0$. Specifically, increasing p_1 or decreasing p_2 does not change the first terms in the formula of Ψ ,

$$\gamma^*(p_1 - p_2) - s_1^{n-1}(p_1 - p_2) = \gamma^*(p_1 + c - p_2) - s_1^{n-1}(p_1 + c - p_2), \quad c \geq 0,$$

since the derivative of $\xi \mapsto \gamma^*(\xi) - s_1^{n-1}\xi$ is constant when $\xi \geq \hat{\xi}$. Setting $\Omega_{\pi}^{n-1} = \{x \in \Omega \mid K_{\pi}^{n-1}(x) = 0\}$ and $\Omega_0^{n-1} = \Omega_1^{n-1} \cup \Omega_2^{n-1}$, it follows that

$$(2.6) \quad \tilde{\Psi}(\mathbf{p}) \equiv \Psi(\mathbf{p}) + \int_{\Omega_0^{n-1}} (1/2) \max(0, p_1 - p_2 - \hat{\xi})^2$$

has the same minima as Ψ and at a minimum $p_2 - p_1 = \hat{\xi}$ on the degenerate sets.

For the example illustrated in Figure 2.2 the slope at the origin is infinite, $\gamma'(0) = -\infty$, so $(\gamma^*)'(\xi) > 0$ on $(-\infty, \hat{\xi})$. If $\gamma'(0)$ were finite, then $(\gamma^*)'(\xi)$ would also vanish on an interval of the form $(-\infty, \hat{\xi})$, and a term of the form $\min(0, p_1 - p_2 + \hat{\xi})^2$ would provide a selection of the pressures on the degenerate sets.

3. If $s_0 = 1$ in a subset of the domain, then $\gamma^*(\xi) = 0$, $s_1 = s_2 = 0$, and both equations for the balance of mass degenerate to zero. Since s_0 is assumed known a priori this case can be eliminated by excising these points from the domain; $\Omega \mapsto \Omega \setminus \bar{\Omega}_0$, where $\Omega_0 = \{x \in \Omega \mid s_0(x) = 1\}$. Below we assume that $s_0 < 1$; however, in a numerical context it may be inconvenient to triangulate $\Omega \setminus \bar{\Omega}_0$, in which case a term of the form $\int_{\Omega_0} p_1^2 + p_2^2$ can be included to eliminate this degeneracy.

In the fully discrete setting, existence and uniqueness of minimizers of control volume approximations of $\tilde{\Psi}$ are established.

2.5. Degenerate convex minimization. While the implicit Euler approximation of the two-phase problem is degenerate, it is not singular. Specifically, Ψ_h and $\tilde{\Psi}_h$ have Lipschitz gradients, and minimizing such functions has been, and continues to be, intensely studied in the optimization community. The numerical examples below utilize the preconditioned Nesterov algorithm [23, 5] with properties summarized in the following theorem.

THEOREM 2.2 (Nesterov). *Let U be a Hilbert space with Riesz map $\mathcal{R} : U \rightarrow U'$, and let $\psi : U \rightarrow \mathbb{R}$ be convex and satisfy*

$$(2.7) \quad (\nabla\psi(v) - \nabla\psi(u), v - u)_U \leq \|v - u\|_U^2.$$

Define the sequence of real numbers $\{\theta_n\}_{n=0}^\infty$ by

$$\theta_n = \frac{1 - \lambda_n}{\lambda_{n+1}}, \quad \text{where } \lambda_0 = 0 \quad \text{and} \quad \lambda_n = \frac{1 + \sqrt{1 + 4\lambda_{n-1}^2}}{2}, \quad n = 1, 2, \dots,$$

and given $u_1 \in U$ define the sequences $\{v_n\}_{n=1}^\infty$ and $\{u_n\}_{n=1}^\infty \subset U$ by $v_1 = u_1$ and

$$v_{n+1} = u_n - g_n, \quad u_{n+1} = (1 - \theta_n)v_{n+1} + \theta_n v_n, \quad \text{with} \quad \mathcal{R}g_n = \nabla\psi(u_n).$$

If $\psi(u_) = \inf_{u \in U} \psi(u)$, then*

$$\psi(v_n) - \psi(u_*) \leq \frac{2\|u_1 - u_*\|_U^2}{n^2} \quad \text{and} \quad \|g_n\|_U \leq \frac{4\|u_1 - u_*\|_U}{n}.$$

The algorithm in this theorem requires inversion of the Riesz map which, in the finite-dimensional context, requires a single LU decomposition of the “stiffness” matrix associated with the inner product $(.,.)_U$. The convex function Ψ in (2.5) is quadratic in the spatial terms, in which case a norm with inner product satisfying the hypothesis (2.7) is

$$\|\mathbf{p}\|_U^2 = \int_\Omega \frac{\beta}{2}(p_1 - p_2)^2 + \frac{\tau}{2} \sum_{\pi=1}^2 |\nabla p_\pi|_{K_\pi^{n-1}}^2,$$

where β is a bound on the second derivative of γ^* .

The preconditioned Nesterov algorithm is robust, and the initial iterates have good descent properties, so we use it to obtain a good initial guess for the Newton-like scheme [15, 27] in Figure 2.3 when more than a few decimal digits are required. This semismooth Newton scheme uses a selection from the Hessian to compute a Newton descent direction, which is then scaled to achieve descent.

3. Spatial approximation. Utilizing a finite-dimensional space of functions for the pressures in (2.4) gives a fully discrete approximation of the two-phase porous flow problem (2.1)–(2.2). Since the continuity properties of the pressures are problem dependent, and may vary with time, spaces which admit discontinuous solutions are natural candidates. In order to focus on the issues that arise with the degeneracies, we assume that the permeability matrices K_π are diagonal and consider the control volume scheme with piecewise constant pressures. This scheme inherits stability estimates identical in structure to those presented for the continuous problem in section 2.3.

```

SEMISSMOOTH NEWTON( $u_0$ )
Initialize:  $\theta = 1$ ,  $\epsilon = 10^{-8}$ ,  $u = u_{old} = u_0$ ,  $\psi_{old} = \psi(u) + 1$ .
while ( $|\nabla\psi(u)| > \epsilon$ )
  if ( $\psi(u) > \psi_{old}$ )
     $\theta = \theta/2$ 
    if ( $\theta < \epsilon$ ) then return (FAIL)
     $u = u_{old} - \theta\delta$ 
  else
     $\psi_{old} = \psi(u)$ ,  $u_{old} = u$ 
    Solve  $(D^2\psi(u) + \epsilon I)\delta = \nabla\psi(u)$ 
     $u = u - \theta\delta$ 
     $\theta = \min(1, 1.25\theta)$ 
return (u)

```

FIG. 2.3. Semismooth Newton scheme for solving $\nabla\psi(u) = 0$.

3.1. Control volume scheme. Given a Delaunay triangulation, \mathcal{T}_h , of the domain $\Omega \subset \mathbb{R}^d$, the control volumes are taken to be the Voronoi regions in Ω associated with each node³ of \mathcal{T}_h . The Voronoi edges/faces (2D/3D) bisect, and are perpendicular to, the edges of \mathcal{T}_h , and the vertices of the Voronoi regions are the circumcenters of the triangles/tetrahedra containing the node. We assume that the circumcircles/circumspheres of the edges/triangles on the boundary of Ω do not contain any nodes in their interior so that the Voronoi regions of nodes on the boundary are well formed [31]; see Figure 3.1.

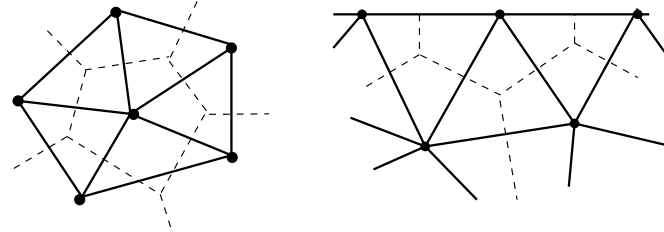


FIG. 3.1. Voronoi regions of interior (left) and boundary (right) nodes.

Integrating (2.4) over a Voronoi cell C_i corresponding to a node of \mathcal{T}_h indexed by i , we obtain

$$\int_{C_i} (s_\pi^n - s_\pi^{n-1}) - \tau \int_{\partial C_i} K_\pi^{n-1} (\nabla p_\pi - \mathbf{b}_\pi) \cdot \mathbf{n} = 0, \quad \pi = 1, 2.$$

Letting \mathcal{N}_i denote the set of nodes connected to i by an edge in \mathcal{T}_h , assuming that $K_\pi = k_\pi I$ is diagonal, and approximating the integrals with one point quadrature rules and derivatives by differences [22, 24] gives

$$(3.1) \quad |C_i|(s_{\pi i}^n - s_{\pi i}^{n-1}) + \tau \sum_{j \in \mathcal{N}_i} \frac{A'_{ij} k_{\pi ij}^{n-1}}{h_{ij}} (p_{\pi i}^n - p_{\pi j}^n + h_{ij} \mathbf{b}_{\pi ij}^{n-1} \cdot \mathbf{n}_{ij}) = 0.$$

³We refer to the points of the triangulation as *nodes* to avoid confusion with the *vertices* of the graph constructed below.

In this expression h_{ij} is the length of the edge from node i to node j , A'_{ij} is the area/length of the dual Voronoi face/edge in 3D/2D, $k_{\pi ij}^{n-1}$ and $\mathbf{b}_{\pi ij}^{n-1}$ are the averages of the permeabilities and body forces at the two nodes, and \mathbf{n}_{ij} is the unit outward vector parallel to the edge. Equation (2.2) is used to compute the saturations \mathbf{s}_i from the pressures \mathbf{p}_i at each node.

Letting \mathcal{N}_h denote the node set and \mathcal{E}_h the edge set of \mathcal{T}_h , equations (3.1) are the Euler–Lagrange equations of the convex function $\Psi_h : \mathbb{R}^{|\mathcal{N}_h|} \times \mathbb{R}^{|\mathcal{N}_h|} \rightarrow \mathbb{R}$ given by

$$\begin{aligned}\Psi_h(\mathbf{p}) = & \sum_{i \in \mathcal{N}_h} |C_i| (\gamma^*(p_{1i} - p_{2i}) - s_{1i}^{n-1}(p_{1i} - p_{2i})) \\ & + \frac{\tau}{2} \sum_{(i,j) \in \mathcal{E}_h} \frac{A'_{ij}}{h_{ij}} \sum_{\pi=1}^2 k_{\pi ij}^{n-1} (p_{\pi i} - p_{\pi j} + h_{ij} \mathbf{b}_{\pi ij}^{n-1} \cdot \mathbf{n}_{ij})^2,\end{aligned}$$

which is the discrete analogue of the function Ψ in (2.5). Solutions of the control volume (3.1) scheme satisfy the stability estimate

$$\begin{aligned}\sum_{i \in \mathcal{N}_h} |C_i| \gamma^*(\mathbf{p}_i^n) + \tau \sum_{m=1}^n \sum_{(i,j) \in \mathcal{E}_h} \frac{A'_{ij}}{h_{ij}} \sum_{\pi=1}^2 k_{\pi ij}^{n-1} (p_{\pi i}^m - p_{\pi j}^m)^2 \leq & \sum_{i \in \mathcal{N}_h} |C_i| \gamma^*(\mathbf{p}_i^0) \\ & + \tau \sum_{m=1}^n \sum_{(i,j) \in \mathcal{E}_h} \frac{A'_{ij}}{h_{ij}} \sum_{\pi=1}^2 k_{\pi ij}^{m-1} (p_{\pi i}^m - p_{\pi j}^m) h_{ij} \mathbf{b}_{\pi ij}^{m-1} \cdot \mathbf{n}_{ij}.\end{aligned}$$

As for the continuous problem, Ψ_h is invariant under translation $(p_1, p_2) \mapsto (p_1 + c, p_2 + c)$ for $c \in \mathbb{R}$. For the prototypical interfacial energy illustrated in Figure 2.2, the arguments in section 2.4 for the continuous problem apply verbatim to the current setting to show that the function

$$(3.2) \quad \tilde{\Psi}_h(\mathbf{p}) = \Psi_h(\mathbf{p}) + \sum_{i \in \mathcal{N}_{0h}^{n-1}} |C_i| \max(0, p_{1i} - p_{2i} - \hat{\xi}_i)^2$$

has the same minimum as Ψ_h , where $\mathcal{N}_{0h}^{n-1} = \mathcal{N}_{1h}^{n-1} \cup \mathcal{N}_{2h}^{n-1}$ with $\mathcal{N}_{\pi h}^{n-1} = \{i \mid k_{\pi ij}^{n-1} = 0, j \in \mathcal{N}_i\}$, and $\hat{\xi}_i$ is the first point where $(\gamma^*)'(\xi_i) = 1 - s_0(x_i)$.

3.2. Existence of solutions. In this section solutions of the control volume scheme (3.1) are constructed as minima of $\tilde{\Psi}_h$. Since $\tilde{\Psi}_h$ is convex on a finite-dimensional space, existence follows from the coercivity condition $\lim_{|\mathbf{p}| \rightarrow \infty} \tilde{\Psi}_h(\mathbf{p}) = \infty$; equivalently, a bound on $\tilde{\Psi}_h(\mathbf{p})$ implies \mathbf{p} is bounded. Coercivity will be established under the following assumptions, which characterize the prototypical interfacial energies and permeabilities illustrated in Figures 2.1 and 2.2 and the meshes illustrated in Figure 3.1.

ASSUMPTION 3.1. $\Omega \subset \mathbb{R}^d$ is a bounded connected domain.

- $s_0 : \Omega \rightarrow [0, 1]$; specifically, $s_0(x) < 1$ for all $x \in \Omega$.
- There exists $C > 0$ such that the permeabilities $k_\pi : \Omega \times [0, 1] \rightarrow \mathbb{R}$ satisfy $0 \leq k_\pi(x, s_\pi) \leq C$ and $k_\pi(x, 0) = 0$. In addition,

$$k_1(x, s_1) + k_2(x, s_2) > 0 \quad \text{when} \quad s_1 + s_2 = 1 - s_0(x).$$

- For each $x \in \Omega$ there exists $\hat{\xi}(x) \in \mathbb{R}$ such that $\gamma^*(x, \cdot) : \mathbb{R} \rightarrow \mathbb{R}$ is convex with derivative strictly increasing on $(-\infty, \hat{\xi}(x))$, and

$$\lim_{\xi \rightarrow -\infty} (\gamma^*)'(x, \xi) = 0 \quad \text{and} \quad (\gamma^*)'(x, \xi) = 1 - s_0(x), \quad \xi \geq \hat{\xi}(x).$$

- \mathcal{T}_h is a Delaunay triangulation of Ω , and the circumballs of boundary simplices do not contain any nodes in their interiors.

THEOREM 3.2. *Let the domain, coefficients, and triangulation satisfy Assumptions 3.1, and let $\tilde{\Psi}_h : \mathbb{R}^{|\mathcal{N}_h|} \times \mathbb{R}^{|\mathcal{N}_h|} \rightarrow \mathbb{R}$ be the convex function in (3.2). Then $\tilde{\Psi}_h$ is coercive on $\{\mathbf{p} \in \mathbb{R}^{|\mathcal{N}_h|} \times \mathbb{R}^{|\mathcal{N}_h|} \mid \sum_{i \in \mathcal{N}_h} |C_i|(p_{1i} + p_{2i}) = 0\}$; in particular, minimizers of $\tilde{\Psi}_h$ exist.*

Proof. Fix $M > 0$ and let $\mathbf{p} : \mathbb{R}^{|\mathcal{N}_h|} \times \mathbb{R}^{|\mathcal{N}_h|} \rightarrow \mathbb{R}$ satisfy $\tilde{\Psi}_h(\mathbf{p}) \leq M$. Assumption 3.1 guarantees that the function $\xi \mapsto \gamma^*(\xi) - s_1^{n-1}\xi$ is bounded below, and since the other terms forming $\tilde{\Psi}_h$ are nonnegative the bound upon $\tilde{\Psi}_h(\mathbf{p})$ implies bounds upon each of them. Specifically, each of the terms

1. $\sum_{i \in \mathcal{N}_h} |C_i| (\gamma^*(p_{1i} - p_{2i}) - s_1^{n-1}(p_{1i} - p_{2i}))$,
2. $\sum_{i \in \mathcal{N}_{2h}^{n-1}} |C_i| \max(0, p_{1i} - p_{2i} - \hat{\xi}_i)^2$, and
3. $\sum_{(i,j) \in \mathcal{E}_h} \frac{A'_{ij}}{h_{ij}} k_{\pi ij}^{n-1} (p_{\pi i} - p_{\pi j})^2$, with $\pi = 1$ and 2,

are bounded. Below we show that these bounds guarantee a bound on the differences $p_{1i} - p_{2i}$ for all $i \in \mathcal{N}_h$. Granted this, the elementary identities

$$\begin{aligned} |p_{1i} - p_{1j}| &\leq |p_{1i} - p_{2i}| + |p_{2i} - p_{2j}| + |p_{2j} - p_{1j}|, \\ |p_{2i} - p_{2j}| &\leq |p_{2i} - p_{1i}| + |p_{1i} - p_{1j}| + |p_{1j} - p_{2j}| \end{aligned}$$

show that the norm

$$|\mathbf{p}|^2 \equiv \sum_{i \in \mathcal{N}_j} |C_i| |p_{1i} - p_{2i}| + \tau \sum_{\pi=1}^2 \sum_{(i,j) \in \mathcal{E}_h} \frac{A'_{ij}}{h_{ij}} (k_{1ij}^{n-1} + k_{2ij}^{n-1}) (p_{\pi i} - p_{\pi j})^2$$

is bounded by a constant depending only upon $M = \tilde{\Psi}_h(\mathbf{p})$. Under the assumptions that Ω is connected and $k_1 + k_2 > 0$, this is a norm on the subspace $\{\mathbf{p} \in \mathbb{R}^{|\mathcal{N}_h|} \times \mathbb{R}^{|\mathcal{N}_h|} \mid \sum_{i \in \mathcal{N}_h} |C_i|(p_{1i} + p_{2i}) = 0\}$, and coercivity follows.

To establish a bound upon the differences $p_{1i} - p_{2i}$ we consider the two cases $0 < s_{1i}^{n-1} < 1 - s_0(x_i)$ and $s_{1i}^{n-1} = 1 - s_0(x_i)$. Note that $s_1 = (\gamma^*)'(p_1 - p_2) > 0$, so these two cases are exhaustive.

- If $0 < s_{1i}^{n-1} < 1 - s_0(x_i)$, Assumption 3.1 shows

$$\lim_{\xi \rightarrow -\infty} \frac{d}{d\xi} (\gamma^*(\xi) - s_{1i}^{n-1}\xi) = -s_{1i}^{n-1} \quad \text{and} \quad \lim_{\xi \rightarrow \infty} \frac{d}{d\xi} (\gamma^*(\xi) - s_{1i}^{n-1}\xi) = 1 - s_0(x_i) - s_{1i}^{n-1}.$$

It follows that $\xi \mapsto \gamma^*(\xi) - s_{1i}^{n-1}\xi$ has linear growth at $\pm\infty$ and so is coercive.

- If $s_{1i}^{n-1} = 1 - s_0(x_i)$, then $\gamma^*(\xi) - s_{1i}^{n-1}\xi$ has linear growth at $-\infty$, so a bound on this term bounds the difference $p_{1i} - p_{2i}$ below by a (typically negative) constant. In addition $s_{2i}^{n-1} = 0$, so $k_2(s_{2i}^{n-1}) = 0$ and $k_1(s_{1i}^{n-1}) > 0$, and thus $k_{1ij}^{n-1} > 0$ for each $j \in \mathcal{N}_i$.

To bound the pressure differences above we consider the following two cases:

- If $k_{2ij}^{n-1} = 0$ for all $j \in \mathcal{N}_i$, then $i \in \mathcal{N}_{2h}^{n-1}$ and the pressure difference is bounded above by $\max(0, p_{1i} - p_{2i} - \hat{\xi}_i)^2$.
- If $k_{2ij}^{n-1} > 0$ for some $j \in \mathcal{N}_i$, then $s_{2j}^{n-1} > 0$, and so $s_{1j}^{n-1} < 1 - s_0(x_j)$ and the previous case then bounds $p_{1j} - p_{2j}$. The elementary identity

$$|p_{1i} - p_{2i}| \leq |p_{1i} - p_{1j}| + |p_{1j} - p_{2j}| + |p_{2j} - p_{2i}|$$

provides a bound on $p_{1i} - p_{2i}$ since $k_{1ij}^{n-1} > 0$ and $k_{2ij}^{n-1} > 0$. \square

Note that this argument only requires the additional term in $\tilde{\Psi}_h$ to include the sum over $i \in \mathcal{N}_{2h}^{n-1}$; summing over $\mathcal{N}_{0h}^{n-1} = \mathcal{N}_{1h}^{n-1} \cup \mathcal{N}_{2h}^{n-1}$ is required for the uniqueness arguments below.

3.3. Uniqueness of minimizers. In this section it is shown that in many instances the additional terms included in $\tilde{\Psi}_h$ are sufficient to select a unique minimum of Ψ_h . While all minima are solutions of the control volume scheme (3.1), and uniqueness is not required by the minimization algorithms presented in section 2.5, elimination of degeneracy in a numerical context and repeatability of numerical computations are desirable.

To establish uniqueness we consider two minimizers, \mathbf{p} and $\tilde{\mathbf{p}}$, of $\tilde{\Psi}_h$. Expanding the identity

$$0 = \tilde{\Psi}_h(\mathbf{p}) + \tilde{\Psi}_h(\tilde{\mathbf{p}}) - 2\tilde{\Psi}_h((1/2)(\mathbf{p} + \tilde{\mathbf{p}})),$$

which follows from convexity of the set of minimizers, shows that

$$(3.3) \quad \begin{aligned} 0 &= \sum_{i \in \mathcal{N}_h} |C_i| \left(\gamma^*(\xi_i) + \gamma^*(\tilde{\xi}_i) - 2\gamma^*((1/2)(\xi_i + \tilde{\xi}_i)) \right) \\ &\quad + \frac{\tau}{4} \sum_{(i,j) \in \mathcal{E}_h} \frac{A'_{ij}}{h_{ij}} \sum_{\pi=1}^2 k_{\pi ij}^{n-1} ((p_{\pi i} - \tilde{p}_{\pi i}) - (p_{\pi j} - \tilde{p}_{\pi j}))^2 \\ &\quad + \sum_{i \in \mathcal{N}_{0h}^{n-1}} |C_i| \left(\max(0, \xi_i - \hat{\xi}_i)^2 + \max(0, \tilde{\xi}_i - \hat{\xi}_i)^2 - 2 \max(0, (1/2)(\xi_i + \tilde{\xi}_i) - \hat{\xi}_i)^2 \right), \end{aligned}$$

where $\xi_i = p_{1i} - p_{2i}$ and $\tilde{\xi}_i = \tilde{p}_{1i} - \tilde{p}_{2i}$. Note that each summand may be identified as a difference quotient for a second derivative for a convex function, and so is nonnegative. That each term vanishes is useful at nodes where the term is strictly convex; at nodes where γ^* has linear growth it is necessary to directly compare $\tilde{\Psi}_h(\mathbf{p})$ and $\tilde{\Psi}_h(\tilde{\mathbf{p}})$.

The following definitions characterize the regions where the spatial terms for each pressure are strictly convex, as well as their overlap.

DEFINITION 3.3. Let \mathcal{T}_h be a triangulation of a domain $\Omega \subset \mathbb{R}^d$, and for $\pi = 1, 2$ let $k_\pi : \mathcal{N}_h \rightarrow [0, \infty)$ be nonnegative functions on the node set of \mathcal{T}_h , $\pi = 1, 2$.

- Two nodes of \mathcal{T}_h are k_π -connected if there is a path in the edge set of \mathcal{T}_h which does not contain two consecutive nodes for which k_π vanishes.
- A k_π -component of \mathcal{N}_h is an equivalence class of the equivalence relation k_π -connectedness.
- The nontrivial k_π -components are those which contain at least one node $v \in \mathcal{N}_h$ for which $k_\pi(v) > 0$, and the set of these components is denoted by \mathcal{V}_π .
- The overlap graph G corresponding to k_1 and k_2 is the graph with vertex set $\mathcal{V}_1 \cup \mathcal{V}_2$, and (V_1, V_2) is in the edge set of G if and only if $V_1 \cap V_2 \neq \emptyset$.

Note that each \mathcal{V}_π is a disjoint partition of a subset of \mathcal{N}_h ; thus an edge in G necessarily has one vertex in \mathcal{V}_1 and one in \mathcal{V}_2 , and so G is bipartite, and vertices $V_\pi \in \mathcal{V}_\pi$ are connected in the sense that for each pair of nodes $m, n \in V_\pi$ there is path in the edge set of \mathcal{T}_h from m to n containing vertices in V_π . Figure 3.2 illustrates the bipartite structure of G where two copies of Ω are represented by the upper and lower lines, with each partitioned into components and degenerate regions \mathcal{N}_{1h}^{n-1} and \mathcal{N}_{2h}^{n-1} . A key observation is that adding a constant to all the pressures $p_{\pi i}$ in a component $V_\pi \in \mathcal{V}_\pi$ does not change the middle (gradient) term in (3.3); coupling with the other component of the pressure is through the interfacial energy γ^* .

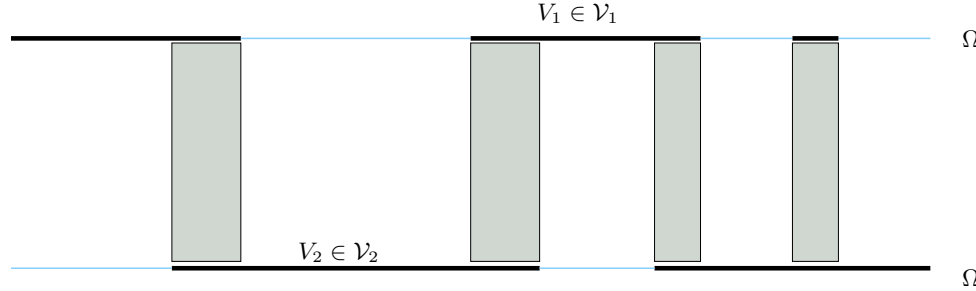


FIG. 3.2. Diagram of the graph G . Heavy lines indicate components in \mathcal{V}_1 (upper) and \mathcal{V}_2 (lower), and light lines show the degenerate regions. Gray areas indicate overlap of nontrivial components.

The following elementary properties of intersecting components will be used below.

LEMMA 3.4. *Let \mathcal{T}_h be a triangulation of a domain $\Omega \subset \mathbb{R}^d$ with node set \mathcal{N}_h , and let G be the overlap graph of two functions $k_\pi : \mathcal{N}_h \rightarrow [0, \infty)$ for which $k_1(n) + k_2(n) > 0$ for every $n \in \mathcal{N}_h$.*

1. *If (V_1, V_2) is an edge in G , then for $\pi = 1, 2$ there exists $n_\pi \in V_1 \cap V_2$ such that $k_\pi(n_\pi) > 0$.*
2. *If Ω is connected, then G is connected.*

Proof.

1. By symmetry it suffices to show there exists $m \in V_1 \cap V_2$ with $k_2(m) > 0$. If $V_2 \subset V_1$, the result is immediate since V_2 , being nondegenerate, contains a vertex with this property. Otherwise, there exist $m' \in V_1 \cap V_2$ and $n' \in V_2 \setminus V_1$, and since V_2 is edge-connected in \mathcal{T}_h there exists an edge (m, n) of \mathcal{T}_h on a path from m' to n' in V_2 for which $m \in V_1 \cap V_2$ and $n \in V_2 \setminus V_1$. Then $k_1(m) = 0$ since $n \in V_1$ otherwise, so $k_2(m) = k_1(m) + k_2(m) > 0$ by hypothesis.
2. When Ω is connected it is immediate that the nodes of the triangulation are edge connected in \mathcal{T}_h . If $V_\pi, V_{\pi'} \in \mathcal{V}_1 \cup \mathcal{V}_2$ are vertices of G , let $n_\pi \in V_\pi$ and $n_{\pi'} \in V_{\pi'}$ be nodes of \mathcal{T}_h . Since \mathcal{T}_h is edge-connected there exists a path from n_π to $n_{\pi'}$ in the edge set of \mathcal{T}_h . Whenever this path exits a component, say $U_1 \in \mathcal{V}_1$, there is an edge (m_1, m_2) of \mathcal{T}_h with $m_1 \in U_1$ and $m_2 \notin U_1$, in which case $k_1(m_2) = 0$; thus $k_2(m_2) > 0$, whence m_2 is in a nondegenerate component $m_2 \in U_2 \in \mathcal{V}_2$. In addition, since $k_2(m_2) > 0$ it follows that $m_1 \in U_2$, so $m_1 \in U_1 \cap U_2$, and hence (U_1, U_2) is an edge in G . Tying together all such edges in G gives a path in G from V_π to $V_{\pi'}$. \square

COROLLARY 3.5. *Let the permeabilities k_π , interfacial energy γ , and triangulation satisfy Assumption 3.1, and let $k_\pi^{n-1} : \mathcal{N}_h \rightarrow \mathbb{R}$ be the functions with values $k_{\pi i}^{n-1} = k_\pi(s_{\pi i}^{n-1})$. Let \mathcal{V}_π be the sets of nontrivial k_π^{n-1} components, and let G denote the corresponding overlap graph.*

If $(V_1, V_2) \in G$ and $\xi : \mathcal{N}_h \rightarrow \mathbb{R}$, then there exists a unique $c \in \mathbb{R}$ at which

$$g(c) = \sum_{i \in V_1 \cap V_2} \gamma^*(\xi_i + c) - s_{1i}^{n-1}(\xi_i + c)$$

is minimal.

Proof. Under Assumption 3.1 g is continuously differentiable with

$$\begin{aligned}\lim_{c \rightarrow -\infty} g'(c) &= - \sum_{i \in V_1 \cap V_2} s_{1i}^{n-1} < 0, \\ \lim_{c \rightarrow \infty} g'(c) &= - \sum_{i \in V_1 \cap V_2} 1 - s_{0i} - s_{1i}^{n-1} = \sum_{i \in V_1 \cap V_2} s_{2i}^{n-1} > 0.\end{aligned}$$

The strict inequalities follow since $k_\pi(0) = 0$, and the lemma guarantees there are nodes where $0 \neq k_{\pi i}^{n-1} = k_\pi(s_{\pi i}^{n-1})$ for $\pi = 1$ and 2. The intermediate value theorem and convexity of g guarantee the existence of an interval $[c_1, c_2]$ upon which g takes its minimal value and g' vanishes.

To establish uniqueness it suffices to show that at a minimum there exists $i \in V_1 \cap V_2$ for which $\xi_i + c < \hat{\xi}_i$ since $\gamma^*(\xi_i + c)$ is strictly convex on $(-\infty, \hat{\xi}_i)$. This is immediate; if $\xi_i + c \geq \hat{\xi}_i$ at every node, then

$$g'(c) = \sum_{i \in V_1 \cap V_2} 1 - s_{0i} - s_{1i}^{n-1} = \sum_{i \in V_1 \cap V_2} s_{2i}^{n-1} > 0,$$

contradicting $g'(c) = 0$. \square

3.4. Fully degenerate case. In the absence of additional assumptions on the permeabilities and surface tension, uniqueness of minimizers of $\tilde{\Psi}_h$ can be established when the domain Ω satisfies the geometric hypotheses in the following theorem.

THEOREM 3.6. *Let $\Omega \subset \mathbb{R}^d$ be a connected domain with $\mathbb{R}^d \setminus \Omega$ connected, and let \mathcal{T}_h be a simplicial triangulation of Ω with node set \mathcal{N}_h . If $k_\pi : \mathcal{N}_h \rightarrow [0, \infty)$ satisfy $k_1(v) + k_2(v) > 0$, then the corresponding overlap graph is a tree.*

The proof of this theorem is presented in the appendix.

THEOREM 3.7. *Let $\Omega \subset \mathbb{R}^d$ be a connected domain with $\mathbb{R}^d \setminus \Omega$ connected, and let \mathcal{T}_h be a Delaunay triangulation of Ω with node set \mathcal{N}_h . If the permeabilities k_π , interfacial energy γ , and triangulation satisfy Assumption 3.1, then minima of the function $\tilde{\Psi}_h : \mathbb{R}^{|\mathcal{N}_h|} \times \mathbb{R}^{|\mathcal{N}_h|} \rightarrow \mathbb{R}$ in (3.2) are unique.*

Proof. Define $k_\pi^{n-1} : \mathcal{N}_h \rightarrow \mathbb{R}$ to be the functions with values $k_{\pi i}^{n-1} = k_\pi(s_{\pi i}^{n-1})$, and let \mathcal{V}_π denote the set of nontrivial k_π^{n-1} components and G denote the corresponding overlap graph characterized in Definition 3.3.

Let \mathbf{p} and $\tilde{\mathbf{p}}$ be two minima of $\tilde{\Psi}$ and write $\xi_i = p_{1i} - p_{2i}$ and $\tilde{\xi}_i = \tilde{p}_{1i} - \tilde{p}_{2i}$. The hypothesis on γ^* and k_π implies $k_{\pi ij}^{n-1} > 0$ for every edge (i, j) of \mathcal{T}_h with nodes $i, j \in V_\pi \in \mathcal{V}_\pi$. Since nodes in the components V_π are connected by edges in \mathcal{T}_h , from (3.3) the following hold:

- The differences $p_{\pi i} - \tilde{p}_{\pi i}$ are constant on components $V_\pi \in \mathcal{V}_\pi$ for $\pi = 1$ and 2.
 - $\xi_i = \tilde{\xi}_i$ on the degenerate set $\mathcal{N}_{0h}^{n-1} = \mathcal{N}_{1h}^{n-1} \cup \mathcal{N}_{2h}^{n-1}$. This follows since $k_{\pi ij}^{n-1} = 0$ if $i \in \mathcal{N}_{\pi h}^{n-1}$, in which case $p_{\pi i}$ and $\tilde{p}_{\pi i}$ are free to minimize $\xi \mapsto \gamma^*(\xi) - s_1^{n-1}\xi + \max(0, \xi - \hat{\xi}_i)^2$, which is strictly convex.
- Note too that if $i \in \mathcal{N}_{\pi h}^{n-1}$, then $k_{\pi i}^{n-1} = 0$, and, since $k_{1i}^{n-1} + k_{2i}^{n-1} > 0$, that $i \in V_{\pi'} \in \mathcal{V}_{\pi'}$, where $\pi' = 1$ if $\pi = 2$, and vice versa. Thus if $p_{\pi'i} = \tilde{p}_{\pi'i}$ on $V_{\pi'}$, then $\xi_i = \tilde{\xi}_i$ implies $p_{\pi i} = \tilde{p}_{\pi i}$; that is, uniqueness on the nondegenerate components implies uniqueness on the degenerate set.

We show that the differences $p_{\pi i} - \tilde{p}_{\pi i}$ take the same constant c on every component $V_\pi \in \mathcal{V}_\pi$ for $\pi = 1$ and 2. Uniqueness then follows since the averages of $p_1 + p_2$ and

$\tilde{p}_1 + \tilde{p}_2$ vanish:

$$0 = \sum_{i \in \mathcal{N}_i} |C_i| ((p_{1i} + p_{2i}) - (\tilde{p}_{1i} + \tilde{p}_{2i})) = 2 \sum_{i \in \mathcal{N}_i} |C_i| c = 2|\Omega|c.$$

Since the overlap graph is connected, it suffices to show that for each pair of components $(V_1, V_2) \in G$ the constant value of $p_{1i} - \tilde{p}_{1i}$ on V_1 is equal to the constant value of $p_{2i} - \tilde{p}_{2i}$ on V_2 .

Fix $(V_1, V_2) \in G$ and write $p_{\pi i} - \tilde{p}_{\pi i} = c_\pi$ for the constant values the differences take on V_π . Then

$$\xi_i - \tilde{\xi}_i = (p_{1i} - p_{2i}) - (\tilde{p}_{1i} - \tilde{p}_{2i}) = c_1 - c_2 \equiv \delta, \quad i \in V_1 \cap V_2.$$

To show that $\delta = 0$ we verify that the function

$$g(c; \xi) = \sum_{i \in V_1 \cap V_2} \gamma^*(\xi_i + c) - s_{1i}^{n-1}(\xi_i + c)$$

is minimized when $c = 0$, and similarly $g(c; \tilde{\xi})$ is minimized when $c = 0$. Since $\xi = \tilde{\xi} + \delta$ on $V_1 \cap V_2$ we find

$$g(c; \xi) = g(c; \tilde{\xi} + \delta) = g(c + \delta; \xi),$$

and the strict convexity of $g(c; \xi)$ at the minimum established in Corollary 3.5 implies $\delta = 0$.

To show that $g(c; \xi)$ is minimized when $c = 0$ we use the property that G is a tree and \mathbf{p} minimizes $\tilde{\Psi}_h(\mathbf{p})$. Since G is a tree, deleting the edge (V_1, V_2) gives two disconnected subtrees, $G \setminus (V_1, V_2) = G_L \cup G_R$, and the subsets of \mathcal{N}_h given by

$$\mathcal{N}_L = \bigcup_{(U_1, U_2) \in G_L} U_1 \cup U_2 \quad \text{and} \quad \mathcal{N}_R = \bigcup_{(U_1, U_2) \in G_R} U_1 \cup U_2$$

have intersection $\mathcal{N}_L \cap \mathcal{N}_R = V_1 \cap V_2$. Define $\mathbf{q} : \mathcal{N}_h \rightarrow \mathbb{R}^2$ by $\mathbf{q}_i = (p_{1i} + c, p_{2i} + c)$ if $i \in \mathcal{N}_R$, and $\mathbf{q}_i = \mathbf{p}_i$ otherwise. Since shifting \mathbf{q} by a constant (\bar{q}, \bar{q}) so that $q_1 + q_2$ averages to zero does not alter $\tilde{\Psi}_h(\mathbf{q})$, and since \mathbf{p} minimizes $\tilde{\Psi}$, it follows that

$$0 \leq \tilde{\Psi}_h(\mathbf{q}) - \tilde{\Psi}_h(\mathbf{p}) = g(c; \xi) - g(0; \xi), \quad c \in \mathbb{R};$$

that is, $c \mapsto g(c; \xi)$ is minimized at $c = 0$. Similarly, since $\tilde{\mathbf{p}}$ also minimizes $\tilde{\Psi}_h$ it follows that $c \mapsto g(c; \tilde{\xi})$ is also minimized at $c = 0$. \square

3.5. Partially degenerate case. The conjugate of the interfacial energy illustrated in Figure 2.2 is nonnegative so that $s_1 = (\gamma^*)'(p_1 - p_2) > 0$ is always nonnegative. If $k_1(s_1)$ only vanishes when $s_1 = 0$, then $k_{1ij}^{n-1} > 0$ for all edges (n_i, n_j) of \mathcal{T}_h , so that \mathcal{V}_1 consists of a single component. In this situation the overlap graph G is a star, and thus is trivially a tree. The requirement that $\mathbb{R}^d \setminus \Omega$ be connected can then be omitted from the hypothesis of Theorem 3.7.

THEOREM 3.8. *Let $\Omega \subset \mathbb{R}^d$ be a connected domain, and let \mathcal{T}_h be a Delaunay triangulation of Ω with node set \mathcal{N}_h . Let the permeabilities k_π , interfacial energy γ , and triangulation satisfy Assumption 3.1, and assume that $k_1(s) = 0$ if and only if $s = 0$. Then minima of the function $\tilde{\Psi}_h : \mathbb{R}^{|\mathcal{N}_h|} \times \mathbb{R}^{|\mathcal{N}_h|} \rightarrow \mathbb{R}$ specified in (3.2) are unique.*

The assumption on k_1 may be relaxed if, for example, a maximum principle is available [21] to establish that s_1 is bounded below by a constant $\hat{s}_1 > 0$ for which $k_1(s) > 0$ when $s \in (\hat{s}_1, 1]$.

4. Well models and nonhomogeneous equations. Naive inclusion of nonhomogeneous terms on the right-hand side of (2.1) gives rise to a term of the form $\mathbf{q} \cdot \mathbf{p}$ in (2.5) for $\Psi(\mathbf{p})$. Since Ψ only has linear growth, this can lead to a loss of existence and uniqueness of minimizers.⁴ In order to model the pressures and fluxes in wells (holes) where fluid may enter and exit, it is common to include a term of the form $W(\mathbf{p}_0 - \mathbf{p})$ at well locations to the right-hand side of (2.1) [11, Chapter 13]. Here the “bottom hole pressure” \mathbf{p}_0 is specified and $W \in \mathbb{R}^{2 \times 2}$ is symmetric and semipositive definite and thus induces a seminorm $|\mathbf{p}|_W^2 = W\mathbf{p} \cdot \mathbf{p}$ on \mathbb{R}^2 . This gives an additional term of the form $Q(\mathbf{p}) = (1/2)|\mathbf{p} - \mathbf{p}_0|_W^2$ on the right-hand side of (2.5) for $\Psi(\mathbf{p})$. Since this term is nonnegative, $\Psi + Q$ is coercive whenever Ψ is, so the existence of solutions follows mutatis mutandis as in Theorem 3.2. However, proofs of uniqueness exploited the invariance of Ψ under translations of the form $(p_1, p_2) \mapsto (p_1 + c, p_2 + c)$ which typically will not hold for $\Psi + Q$.

5. Numerical example. A numerical example with prototypical fluid and medium properties and significant degeneracy is presented to illustrate the robustness of the formulation. Nondimensionalizing equations (2.1) with characteristic time $T = 10^7 s$ (a year), length $L = 10^3 m$ (kilometers), and pressure $P = 10^6 Pa$, gives nondimensional equations of the same form with the permeability scaled by $TP/L^2 = 10^7$. For prototypical geological problems [13] the permeability of the medium is $K = O(10^{-10})m^2$ and fluid viscosities $\mu = O(10^{-3})Pa\,s$, so the permeability $k \simeq K/\mu$ for the nondimensional equations is of order $O(1)$. With this scaling, all computed quantities are well centered in the floating point range. The following parameters were selected to model a layered medium in a two-kilometer-square domain, $\Omega = [-1, 1]^2$, with an impermeable depression of radius $\ln(1.25)/2 \simeq 0.11$ centered at $c = (1/4, -1/4)$. An injection well is located in the lower left corner $(-1, -1)$ and production at the upper right corner $(1, 1)$.

- Domain: $[-1, 1]^2$ with $0 \leq t \leq T = 5$.
- Boundary data: No flux for each fluid.
- Volume ratio of medium: $s_0(x) = 0.7 + 0.1 \sin(2x_1 + x_2)$, porosity $\phi = 1 - s_0$.
- Medium permeability: $K_0/\mu = 2.5 \max(\exp(|x - c|^2) - 1.25, 0)I$, with $c = (1/4, -1/4)$ and viscosities for each fluid taken to be the same, $\mu = \mu_1 = \mu_2$.
- Phase permeabilities: $K_\pi(s_\pi) = s_\pi \max(0, s_\pi - 0.1(1 - s_0))K_0$.
- Wells: $Q(x, \mathbf{p}) = (1/2)(p_1 - 60)^2 \chi_{B_{1/8}(-1, -1)}(x) + (1/2)|\mathbf{p}|^2 \chi_{B_{1/8}(1, 1)}(x)$.
- Interfacial energy: With $p^* \equiv -1/(2\sqrt{1 - s_0})$ and $s_0 = s_0(x)$ as above,

$$\gamma^*(p_1 - p_2) = \begin{cases} (1 - s_0)(p_1 - p_2), & p_1 - p_2 \leq p^*, \\ -1/(4(p_1 - p_2)) - \sqrt{1 - s_0} & \text{otherwise.} \end{cases}$$

This is the conjugate function from Example 1.

- Initial data: $\mathbf{s} = \partial(I_L + \Gamma)^*(\mathbf{p})$, where $\mathbf{p} = (-5, 5)$ is computed with (2.2).

Figure 5.1 illustrates the saturation of the injected fluid obtained with this data at three times:

- Left: The injected fluid is forced towards the top around the impervious region.
- Middle: The injected fluid reaches the production well (breakout). The layered medium has porosity in the range $0.2 \leq 1 - s_0 \leq 0.4$, and the injected fluid has saturated the pores in the lower left portion of the domain.

⁴The prototypical example is $\Psi(p) = |p| - qp$ for $p \in \mathbb{R}$. If $|q| < 1$, minimizers exist and are unique; if $|q| = 1$, minimizers exist but are not unique; and when $|q| > 1$, there are no minimizers.

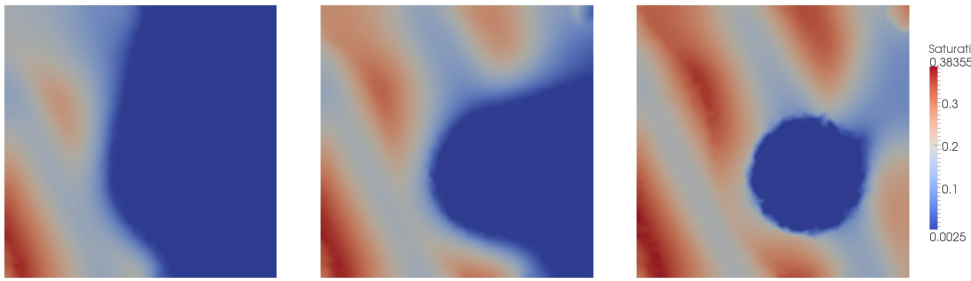


FIG. 5.1. *Saturations of injected fluid at times $t = 1, 1.75, 5$.*

- Right: At the final time the injection fluid has surrounded the impenetrable region and is slowly displacing residual amounts of the second fluid from the narrow region on the right. The injected fluid forms the majority of fluid emanating from the production well.

This solution was computed using 512 time steps ($\tau = 5/512$) on a Delaunay mesh [34] with 1592 vertices (two pressures per vertex) and 3061 triangles. The solution at each step was computed as a minima of the convex function $\tilde{\Psi}_h$ given in (3.2) using 50 Nesterov iterations to obtain an initial approximation for the semismooth Newton scheme of Figure 2.3 which, for this example, then converged in 3–5 iterations.

Appendix A. Proof of Theorem 3.6. The proof of the tree property of overlap graphs utilizes multiple notions of connectedness.

NOTATION A.1. *Triangulations of a domain will be denoted by \mathcal{T} and the node set by \mathcal{N} . We write $K \in \mathcal{T}$ if K is a simplex (node, edge, ...) of \mathcal{T} .*

- $A \subset \mathbb{R}^d$ is connected if it cannot be covered by two disjoint open sets. Open sets in \mathbb{R}^d are locally path connected, so if A is open it is connected if and only if it is path connected.
- $\mathcal{A} \subset \mathcal{N}$ is edge connected (in \mathcal{T}) if for any two nodes in \mathcal{A} there is a path from one to the other in the edge set of \mathcal{T} with nodes in \mathcal{A} .
- Given functions $k_\pi : \mathcal{N} \rightarrow \mathbb{R}$, the notion of k_π connectedness of Definition 3.3 is utilized.

Note that if $\mathcal{A} \subset \mathcal{N}$ is k_π connected, then it is edge connected.

These are all equivalence relations and so give rise to disjoint partitions into (maximally)⁵ connected components.

The proof of Theorem 3.6 uses the following simple but subtle theorem from algebraic topology [14].

THEOREM A.2. *Let $A \subset \mathbb{R}^d$ be open and connected. The complement $A^c = \mathbb{R}^d \setminus A$ is connected if and only if the boundary ∂A of A is connected.*

The following lemma is a discrete analogue of the nontrivial implication of this theorem. In this lemma the distance $d(m, n)$ between nodes in \mathcal{N} is the least number of edges in a path in the edge set of \mathcal{T} connecting them.

LEMMA A.3. *Let \mathcal{T} be a simplicial triangulation of \mathbb{R}^d with node set \mathcal{N} , and let $d(m, n) \in \mathbb{N}$ denote the distance between nodes in the edge set of \mathcal{T} . If $\mathcal{A} \subset \mathcal{N}$ is an*

⁵The maximal property of components follows from their definition as equivalence classes. The redundant use of *maximal* is used when it is the essential property for an argument.

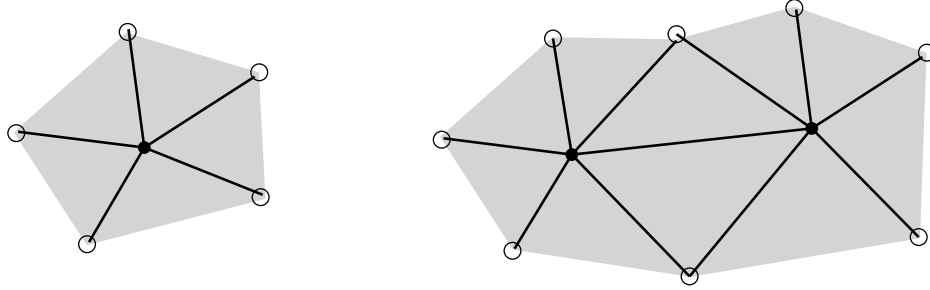


FIG. A.1. *Proof of Lemma A.3: neighborhood of $n \in \mathcal{A}$ (left) and two adjacent points in \mathcal{A} (right).*

edge connected set of nodes and the complement $\mathcal{A}^c = \mathcal{N} \setminus \mathcal{A}$ is also edge connected, then the set of nodes $d_1(\mathcal{A}) \equiv \{n \in \mathcal{N} \mid d(n, \mathcal{A}) = 1\}$ is edge connected. That is, if $m, n \in d_1(\mathcal{A})$, then there is a path of edges in \mathcal{T} from m to n with nodes in $d_1(\mathcal{A})$.

Proof. In order to use Theorem A.2 we define the open set (see Figure A.1)

$$A = \mathcal{A} \cup \bigcup_{n \in \mathcal{A}} \{\overset{\circ}{K} \mid n \in K, K \text{ a simplex in } \mathcal{T}\} \subset \mathbb{R}^d.$$

Here $\overset{\circ}{K}$ denotes the interior of a simplex (edge, triangle, tetrahedron) K . To show that A and $A^c \equiv \mathbb{R}^d \setminus A$ are connected we use the property that $\mathcal{N} \cup_{K \in \mathcal{T}} \overset{\circ}{K}$ is a disjoint partition of \mathbb{R}^d . Then the following hold:

- If (m, n) is an edge in \mathcal{T} with $m, n \in \mathcal{A}$, then the segment $[m, n] \subset A$ by construction. Conversely, if $m, n \in \mathcal{A}^c$, then the open segment $(m, n) \not\subset A$, so $[m, n] \subset A^c$. By the hypothesis, \mathcal{A} is edge connected, and thus any two vertices in \mathcal{A} are connected by a path in A ; similarly, two nodes in \mathcal{A}^c are connected by a path in A^c .
- Every point $x \in \mathbb{R}^d \setminus \mathcal{N}$ is in the interior of a simplex $K \in \mathcal{T}$. If K contains a node in \mathcal{A} , then $x \in \overset{\circ}{K} \subset A$; otherwise, $x \in K \subset A^c$. Since $\overset{\circ}{K}$ is convex there is a path $[x, n] \subset \overset{\circ}{K}$ from x to any node $n \in \partial K$.
- It follows that any two points $x, y \in A$ (resp., A^c) can be connected by a path of the form $[x, m] \cup [m, n] \cup (n, y) \subset A$ (resp., $\subset A^c$), with m and n nodes of \mathcal{A} (resp., \mathcal{A}^c).

Theorem A.2 then shows that the (topological) boundary ∂A of A is connected. We next show that $\mathcal{N} \cap \partial A = \{n \in \mathcal{T} \mid d(n, \mathcal{A}) = 1\}$.

Superset: $\mathcal{N} \cap \partial A \supset d_1(\mathcal{A})$. If $d(n, \mathcal{A}) = 1$, then there exists an edge $[m, n]$ of \mathcal{T} with $m \in \mathcal{A}$. Then $[m, n] \subset A$ so $n \in \partial A$.

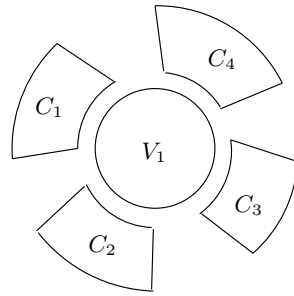
Containment: $\mathcal{N} \cap \partial A \subset d_1(\mathcal{A})$. Since A is open it follows that $A \cap \partial A = \emptyset$, and so it is immediate that $d(n, \mathcal{A}) > 0$ when $n \in \mathcal{N} \cap \partial A$; we show $d(n, \mathcal{A}) < 2$.

Let $n \in \mathcal{N}$ with $d(n, \mathcal{A}) \geq 2$, and let K be a simplex containing it; $n \in K \in \mathcal{T}$. Since $d(m, n) = 1$ for every node $m \in K$ it follows from the triangle inequality that $m \notin \mathcal{A}$, and so $\overset{\circ}{K} \not\subset A$. Then

$$\{n\} \cup \{\overset{\circ}{K} \mid n \in K, K \text{ a simplex in } \mathcal{T}\} \subset A^c$$

is an open neighborhood of n disjoint from A ; in particular, $n \notin \partial A$.

To conclude that $d_1(\mathcal{A})$ is edge connected it suffices to show $\{K \subset \partial A \mid K \in \mathcal{T}\}$ is a triangulation of ∂A . If $x \in \partial A \setminus \mathcal{N}$, let $K \in \mathcal{T}$ be the (unique) simplex for which $x \in \overset{\circ}{K}$.

FIG. A.2. Partition of node set \mathcal{N} in the proof of Theorem A.4.

- K does not have a node in \mathcal{A} since otherwise $x \in \overset{\circ}{K} \subset A$.
- Since $x \in \partial A$ every neighborhood of x intersects A ; in particular, $x \in \partial K'$ for some d simplex with $\overset{\circ}{K}' \subset A$. (If $\overset{\circ}{k} \subset A$ and $k \subset K'$, then $\overset{\circ}{K}' \subset A$.) Since \mathcal{T} is a triangulation, it follows that $K \subset K'$ (a d simplex contains any subsimplex that it intersects).
- It follows that $K \subset \bar{A}$ and does not contain a node of \mathcal{A} ; thus $K \not\subset A$, whence $K \subset \bar{A} \setminus A = \partial A$. \square

We first prove the tree property when $\Omega = \mathbb{R}^d$; the proof of Theorem 3.6 will then be deduced from this.

THEOREM A.4. *Let \mathcal{T}_h be a simplicial triangulation of \mathbb{R}^d with node set \mathcal{N}_h . If $k_\pi : \mathcal{N}_h \rightarrow [0, \infty)$ satisfy $k_1(v) + k_2(v) > 0$, then the corresponding overlap graph G is a tree.*

Proof. Suppose to the contrary that G contains a cycle. Then there exist vertices $V_1, \tilde{V}_1 \in \mathcal{V}_1$ of G and paths P and \tilde{P} from V_1 to \tilde{V}_1 in G for which the end points are the only vertices in common. We establish a contradiction by showing that there is a vertex $V_2 \in \mathcal{V}_2$ of G common to both paths.

Let C_1, C_2, \dots, C_M be the edge connected components of $\mathcal{N} \setminus V_1$. Then $V_1 \cap \tilde{V}_1 = \emptyset$, and so $\tilde{V}_1 \subset \mathcal{N} \setminus V_1$ and \tilde{V}_1 is edge connected; thus, without loss of generality, assume $\tilde{V}_1 \subset C_1$. Since the components are pairwise disjoint it follows that

$$C_1^c \equiv \mathcal{N} \setminus C_1 = V_1 \cup \bigcup_{i=2}^M C_i;$$

moreover, this is a disjoint partition (see Figure A.2).

Claim. C_1^c is an edge connected subset of \mathcal{N} .

Proof. For any two nodes $n \in V_1$ and $m \in C_i$ there exists a path p in the edge set of \mathcal{T} joining them. Since the C_i are (maximally) edge connected components, there are no edges between any two of them, and thus the subpath p' of p starting with the last edge to enter C_i is a path from some $n' \in V_1$ to m and is contained in $V_1 \cup C_i$. Since V_1 is edge connected it follows there is a path q from n to n' in V_1 . Then $q + p'$ is a path from n to m in $V_1 \cup C_i$, and since $i \geq 2$ is arbitrary the claim follows. \square

Then C_1 and C_1^c are edge connected subsets of \mathcal{N} , and it follows from the previous lemma that $d_1(C_1^c) \equiv \{n \in \mathcal{N} \mid d(n, C_1^c) = 1\}$ is edge connected.

Claim. $d_1(C_1^c) \subset d_1(V_1)$.

Proof. If $d(n, C_1^c) = 1$, there exists an edge (m, n) in \mathcal{T} for which $n \in C_1$ and $m \in C_1^c$. Since $\{C_i\}$ are (maximally) connected edge components, there are no edges between them; in particular, $d(m, n) > 1$ for any $m \in \cup_{i=2}^M C_i$. It then follows that $m \in V_1$. \square

To complete the proof, suppose V_1 and $\tilde{V}_1 \in \mathcal{V}_1$ are distinct vertices of G and there exist paths P and P' in the edge set of G connecting them which intersect only at the end points. Since k_π components are edge connected in \mathcal{T} , it follows from the definition of the overlap graph that for any $m \in V_1$ and $n \in \tilde{V}_1$ there exist paths p and p' in the edge set of \mathcal{T} from m to n which only intersect in V_1 and \tilde{V}_1 .

Since $V_1 \subset C_1^c$ and $\tilde{V}_1 \subset C_1$, each path p and p' must exit C_1 ; in particular, there are edges (m, n) and (m', n') on these paths for which $m, m' \in C_1$ and $n, n' \notin C_1$ so that $d(n, C_1) = d(n', C_1) = 1$.

Since V_1 is a (maximally) k_1 connected component it follows that $k_1(i) = 0$ for any vertex for which $d_1(i, V_1) = 1$, and hence $k_2(i) > 0$. In particular, $k_2(i) > 0$ for every vertex $i \in d_1(C_1)$ and $d_1(C_1)$ is also edge connected, so that $d_1(C_1) \subset V_2$ for some k_2 component $V_2 \in \mathcal{V}_2$.

The contradiction now follows since $n \in V_2$ and $n' \in V_2$ show that V_2 is a vertex of G on each path from V_1 to \tilde{V}_1 . \square

Proof of Theorem 3.6. Let \mathcal{T} be a triangulation of a connected domain $\Omega \subset \mathbb{R}^d$, let $k_\pi \rightarrow [0, \infty)$ satisfy $k_1(n) + k_2(n) > 0$ at every node of \mathcal{T} , and let G denote the corresponding overlap graph. Extending \mathcal{T} to a triangulation \mathcal{T}' of \mathbb{R}^d setting $k_\pi(n) = 1/2$ for nodes n not in \mathcal{T} gives a triangulation and functions satisfying the hypothesis of the previous theorem so that the overlap graph G' for the extended triangulation and functions is a tree. Since k_π components of \mathcal{N} are contained in k_π components of \mathcal{N}' it follows that G is a subgraph of G' , and thus is a forest. However, Lemma 3.4 shows that G is connected, and so it is a tree. \square

REFERENCES

- [1] H. W. ALT AND E. DIBENEDETTO, *Nonsteady flow of water and oil through inhomogeneous porous media*, Ann. Scuola Norm. Sup. Pisa Cl. Sci. (4), 12 (1985), pp. 335–392.
- [2] T. ARBOGAST, *The existence of weak solutions to single porosity and simple dual-porosity models of two-phase incompressible flow*, Nonlinear Anal., 19 (1992), pp. 1009–1031.
- [3] T. ARBOGAST, M. JUNTUNEN, J. POOL, AND M. F. WHEELER, *A discontinuous Galerkin method for two-phase flow in a porous medium enforcing $H(\text{div})$ velocity and continuous capillary pressure*, Comput. Geosci., 17 (2013), pp. 1055–1078.
- [4] R. H. BROOKES AND A. T. COREY, *Hydraulic Properties of Porous Media*, Hydrology Paper 3, Department of Civil Engineering, Colorado State University, Fort Collins, CO, 1964.
- [5] S. BUBECK, *Orf523: Nesterov's Accelerated Gradient Descent*, <https://blogs.princeton.edu/imabandit/2013/04/01/acceleratedgradientdescent/>, 2013.
- [6] C. CANCEËS, T. O. GALLOUËT, AND L. MONSAINGEON, *Incompressible immiscible multiphase flows in porous media: A variational approach*, Anal. PDE, 10 (2017), pp. 1845–1876.
- [7] C. CANCEËS, I. S. POP, AND M. VOHRALÍK, *An a posteriori error estimate for vertex-centered finite volume discretizations of immiscible incompressible two-phase flow*, Math. Comp., 83 (2014), pp. 153–188.
- [8] G. CHAVENT AND J. JAFFRE, *Mathematical Models and Finite Elements for Reservoir Simulation*, North-Holland, Amsterdam, 1986.
- [9] Z. CHEN, *Degenerate two-phase incompressible flow. I. Existence, uniqueness and regularity of a weak solution*, J. Differential Equations, 171 (2001), pp. 203–232.
- [10] Z. CHEN AND R. E. EWING, *Degenerate two-phase incompressible flow. III. Sharp error estimates*, Numer. Math., 90 (2001), pp. 215–240.
- [11] Z. CHEN, G. HUAN, AND Y. MA, *Computational Methods for Multiphase Flows in Porous Media*, Comput. Sci. Eng. 2, SIAM, Philadelphia, PA, 2006, <https://doi.org/10.1137/1.9780898718942>.

- [12] Z. CHEN AND N. L. KHLOPINA, *Degenerate two-phase incompressible flow problems. II. Error estimates*, Commun. Appl. Anal., 5 (2001), pp. 503–521.
- [13] A. CHENG, *Poroelasticity*, Theory Appl. Transp. Porous Media 27, Springer, Cham, 2016.
- [14] A. CZARNECKI, M. KULCZYCKI, AND W. LUBAWSKI, *On the connectedness of boundary and complement for domains*, Ann. Polon. Math., 103 (2012), pp. 189–191.
- [15] J. E. DENNIS, JR., AND J. J. MORÉ, *Quasi-Newton methods, motivation and theory*, SIAM Rev., 19 (1977), pp. 46–89, <https://doi.org/10.1137/1019005>.
- [16] J. DOUGLAS, D. PEACEMAN, AND H. RACHFORD, *A method for calculating multi-dimensional immiscible displacement*, Petroleum Trans., 216 (1959), pp. 297–308.
- [17] J. DOUGLAS, M. PESZYNNSKA, AND R. E. SHOWALTER, *Single phase flow in partially fissured media*, Transp. Porous Media, 28 (1997), pp. 285–306.
- [18] R. EYMARD, R. HERBIN, AND A. MICHEL, *Mathematical study of a petroleum-engineering scheme*, M2AN Math. Model. Numer. Anal., 37 (2003), pp. 937–972.
- [19] B. GANIS, K. KUMAR, G. PENCHEVA, M. F. WHEELER, AND I. YOTOV, *A global Jacobian method for mortar discretizations of a fully implicit two-phase flow model*, Multiscale Model. Simul., 12 (2014), pp. 1401–1423, <https://doi.org/10.1137/140952922>.
- [20] R. JORDAN, D. KINDERLEHRER, AND F. OTTO, *The variational formulation of the Fokker-Planck equation*, SIAM J. Math. Anal., 29 (1998), pp. 1–17, <https://doi.org/10.1137/S0036141096303359>.
- [21] D. KROENER AND S. LUCKHAUS, *Flow of oil and water in a porous medium*, J. Differential Equations, 55 (1984), pp. 276–288.
- [22] G. L. MILLER, D. TALMOR, S.-H. TENG, AND N. WALKINGTON, *On the radius-edge condition in the control volume method*, SIAM J. Numer. Anal., 36 (1999), pp. 1690–1708, <https://doi.org/10.1137/S0036142996311854>.
- [23] Y. E. NESTEROV, *A method for solving the convex programming problem with convergence rate $O(1/k^2)$* , Dokl. Akad. Nauk SSSR, 269 (1983), pp. 543–547.
- [24] R. A. NICOLAIDES, *Direct discretization of planar div-curl problems*, SIAM J. Numer. Anal., 29 (1992), pp. 32–56, <https://doi.org/10.1137/0729003>.
- [25] F. OTTO, *The geometry of dissipative evolution equations: The porous medium equation*, Comm. Partial Differential Equations, 26 (2001), pp. 101–174.
- [26] M. PESZYNNSKA, Q. LU, AND M. F. WHEELER, *Coupling different numerical algorithms for two phase fluid flow*, in The Mathematics of Finite Elements and Applications X, J. Whiteman, ed., Elsevier, 1999, pp. 205–214.
- [27] L. QI AND D. SUN, *A survey of some nonsmooth equations and smoothing Newton methods*, in Progress in Optimization, Appl. Optim. 30, Kluwer Academic, Dordrecht, 1999, pp. 121–146.
- [28] F. A. RADU, K. KUMAR, J. M. NORDBOTTEN, AND I. S. POP, *A robust, mass conservative scheme for two-phase flow in porous media including Hölder continuous nonlinearities*, IMA J. Numer. Anal., 38 (2018), pp. 884–920.
- [29] B. RIVIÈRE, *Discontinuous Galerkin Methods for Solving Elliptic and Parabolic Equations. Theory and Implementation*, Frontiers Appl. Math. 35, SIAM, Philadelphia, PA, 2008, <https://doi.org/10.1137/1.9780898717440>.
- [30] R. T. ROCKAFELLAR, *Lagrange multipliers and optimality*, SIAM Rev., 35 (1993), pp. 183–238, <https://doi.org/10.1137/1035044>.
- [31] J. RUPPERT, *A new and simple algorithm for quality 2-dimensional mesh generation*, in Third Annual ACM-SIAM Symposium on Discrete Algorithms, ACM, New York, SIAM, Philadelphia, PA, 1992, pp. 83–92.
- [32] B. SAAD AND M. SAAD, *A combined finite volume-nonconforming finite element scheme for compressible two phase flow in porous media*, Numer. Math., 129 (2015), pp. 691–722.
- [33] B. SEQUIN AND N. J. WALKINGTON, *Multi-component multiphase flow*, Archive for Rational Mechanics and Analysis, submitted.
- [34] J. R. SHEWCHUK, *Triangle 1.6, A Two-Dimensional Quality Mesh Generator and Delaunay Triangulator*, <http://www.cs.cmu.edu/~quake/triangle.html>, 2005.
- [35] R. E. SHOWALTER, *Monotone Operators in Banach Space and Nonlinear Partial Differential Equations*, AMS, Providence, RI, 1997; available online from <http://www.ams.org/online-bks/surv49/>.
- [36] M. VOHRALÍK AND M. F. WHEELER, *A posteriori error estimates, stopping criteria, and adaptivity for two-phase flows*, Comput. Geosci., 17 (2013), pp. 789–812.